JACS
JOURNAL OF THE AMERICAN CHEMICAL SOCIETY
Article
pubs.acs.org/JACS

Two-Dimensional Phosphorus Porous Polymorphs with Tunable Band Gaps

Zhiwen Zhuo,[†,‡] Xiaojun Wu,*[,†,‡,§] and Jinlong Yang[†,§]

[†]CAS Key Laboratory of Materials for Energy Conversion, School of Chemistry and Materials Sciences, and CAS Center for Excellence in Nanoscience, [‡]Hefei National Laboratory of Physical Sciences at the Microscale, and [§]Synergetic Innovation of Quantum Information & Quantum Technology, University of Science and Technology of China, Hefei, Anhui 230026, China

Supporting Information

ABSTRACT: Exploring stable two-dimensional (2D) crystalline structures of phosphorus with tunable properties is of considerable importance partly due to the novel anisotropic behavior in phosphorene and potential applications in high-performance devices. Here, 21 new 2D phosphorus allotropes with porous structure are reported based on topological modeling method and first-principles calculations. We establish that stable 2D phosphorus crystals can be obtained by topologically assembling selected phosphorus monomer, dimer, trimer, tetramer, and hexamer. Nine of reported structures are predicted to be more stable than white phosphorus. Their dynamic and thermal stabilities are confirmed by the calculated vibration spectra and Born−Oppenheimer molecular dynamic simulation at temperatures up to 1500 K. These phosphorus porous polymorphs have isotropic mechanic properties that are significantly softer than phosphorene. The electronic band structures calculated with the HSE06 method indicate that new structures are semiconductors with band gaps ranging widely from 0.15 to 3.42 eV, which are tuned by the basic units assembled in the network. Of particular importance is that the position of both conduction and valence band edges of some allotropes matches well with the chemical reaction potential of H_2/H^+ and O_2/H_2O, which can be used as element photocatalysts for visible-light-driven water splitting.

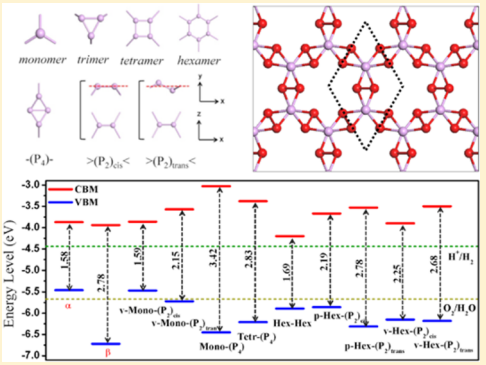

INTRODUCTION

Since the discovery of graphene in 2004,[1] exploring additional two-dimensional (2D) crystals with widely tunable properties, such as bang gap, has attracted tremendous interest either for fundamental research or practical applications in high-performance electronic and optoelectronic devices. Except for various graphene-like inorganic compounds,[2−4] of particular interest are single-element-based sheets, which possibly possess rich 2D allotropic structures as their bulk counterparts with versatile properties related to the arrangements of atoms in 2D networks.[5−19] For example, carbon has versatile bonding characteristics and various allotropes in nature ranging from graphite to graphene. Since the discovery of graphene, a big family of 2D carbon allotropes with mixtures of sp, sp^2, and sp^3-hybridized carbon in networks has been reported theoretically and experimentally.[5−10] Particularly, remarkable properties, such as moderate-size band gap,[5] high catalytic activity,[20] anisotropic Dirac behavior,[21] inherent ferromagnetism,[22] potential superconductivity,[23] and ultrahigh ideal strength,[7] are predicted in some 2D carbon allotropes that even outperform graphene. Another example is the element boron. Theoretical works have predicted that boron has multiple 2D allotropes due to its distinct capability to form multicovalent bonds with itself.[24−28] Experimentally, flat boron clusters and nanosheets have been realized very recently.[29−32]

Phosphorus is a group-V element with typical 3-fold coordination. Experimentally, phosphorus also has a large number of allotropes ranging from black phosphorus,[33] α-, β-, γ-phases of white phosphorus,[34] violet or Hittorf's,[35] fibrous,[36] to some kinds of nanorods phases[37] belonging to so-called red phosphorus. Recently, the successful fabrication of phosphorene[38−40] (also named as α-P), a single layer of black phosphorus, has attracted intense attention for its novel properties distinctly different from other 2D materials.[38−42] With a unique puckered structure, phosphorene exhibits novel anisotropic physical[38,43−49] and mechanical properties,[50−53] such as anisotropic thermoelectric,[46−49] topological insulator,[54] superconductivity,[55] integer quantum Hall effect,[56] negative Possion's ratio,[51−53] and promising applications in electronics,[38−40] energy storage,[57−61] photovoltaic,[62,63] and gas sensors.[64] Therefore, it is of profound interest to explore new 2D phosphorus allotropes complementary to phosphorene with tunable properties.

In the past years, many 2D phosphorus allotropes with compacted honeycomb or nonhoneycomb structures have been proposed from first-principles calculations, including blue phosphorene (β-P),[65] γ-P, δ-P,[66] h-θ-P,[67] ε-P, ζ-P, η-P, θ-P,[68] red phosphorene,[69] three novel structures with 2-, 3-, and 4-fold

Received: March 21, 2016
Published: May 12, 2016

ACS Publications © 2016 American Chemical Society

DOI: 10.1021/jacs.6b02964
J. Am. Chem. Soc. 2016, 138, 7091−7098

coordination (α-P_6, β-P_6, and 558-P_6),[70] some special structures noted as 4−8-, 3−12- (or Kakome P),[71] 5−7-, 5−8-P by their membered rings,[67] and five very stable structures B1, B2, G1, G2, and G3 proposed by gene recombination methods.[72] Among them, β-P, γ-P, δ-P, h-θ-P, and red phosphorene have honeycomb structures, as does α-P, that they can be transformed into each other without bonds broken.[65] All 2D allotropes are semiconductors, and α-P, ε-P, and α-P_6 have direct band gaps of 1.59, 0.94, and 1.36 eV, respectively.[69,70]

Here we report 21 new 2D phosphorus allotropes with porous structures by assembling phosphorus monomer, dimer, trimer, tetramer, and hexamer based on topological method and first-principles calculations. Nine of them are predicted to be more stable than white phosphorus ranked based on the calculated energy. Both crystal and thermal stabilities are confirmed by the calculated phonon spectrum and Born−Oppenheimer molecular dynamics simulations at high temperature up to 1500 K. These allotropes are semiconductors with widely tunable band gap ranging from 0.15 to 3.42 eV. In particular, the band structures of eight 2D phosphorus allotropes, that have a moderate-size band gap starting from 1.69 eV, match well with the chemical reaction potential of H_2/H^+ and O_2/H_2O. These results demonstrate their potential applications as element photocatalysts for visible-light-driven overall water splitting that might outperform α-P and violet phosphorus.[41,73]

COMPUTATIONAL DETAILS

All calculations are carried out with density functional theory (DFT) method implemented in Vienna ab initio simulation package (VASP).[74] The projector augmented wave (PAW) method[75] is applied to describe the electron−ion interaction, and plane-waved energy cutoff is 500 eV with treatment of valence electron on element phosphorus in configuration of $3s^23p^3$. The exchange−correlation interaction functional is the generalized gradient approximation (GGA) in Perdew, Burke, and Ernzerhof (PBE) functional.[76] Note that because pure DFT always underestimates the band gap of semiconductors, the Heyd, Scuseria, and Ernzerhof (HSE06)[77] screened hybrid density functional method is used to obtain the electronic structures. The convergences of force between atoms for optimization and total energy for wave function self-consistent are set to 0.01 eV/Å and 10^{-6} eV, respectively. The vacuum size is chosen as 20 Å to avoid interaction between two layers for all structures. The first Brillouin zone integration using Γ-center scheme is sampled with a k-point separation of <0.02 $Å^{-1}$ for optimization and <0.01 $Å^{-1}$ for energy calculation. Specifically, the k-points setting is 15 × 15 × 1, 9 × 9 × 1 for small hexagonal cells (<7 Å) and large hexagonal cell (>8 Å) and 16 × 16 × 1 and 10 × 10 × 1 for small tetragonal cells (<7 Å) and large tetragonal cell (>8 Å) to obtain static total energy and properties, respectively. For photon absorption calculation in HSE06 method, k-point is 9 × 9 × 1 for v-Mono-$(P_2)_{trans}$ and Mono-(P_4) and 5 × 5 × 1 for large systems including v-Hex-$(P_2)_{trans}$, v-Hex-$(P_2)_{trans}$ p-Hex-$(P_2)_{ci}$, p-Hex-$(P_2)_{trans}$, and Tetr-(P_4). The phonon spectrum calculation is obtained with finite displacement method implemented in CASTEP package.[78] A plane-wave energy cutoff of 400 eV with ultrasoft pseudopotential is used. Born−Oppenheimer molecular dynamic simulation (BOMD) is performed at the DFT level for selected systems. The constant volume and constant temperature ensemble (NVT) is used. The time step is 1 fs, and the total simulation time is 5 ps. To consider the effect of layer−layer interaction, DFT-D2 method[79] with van der Waals force correction is employed to simulate bilayer structure. Additionally, G-SSNEB method[80] is employed to estimate the activation energy for transformation between structures with the force convergence of 0.02 eV/Å.

RESULTS AND DISCUSSION

To enumerate possible 2D phosphorus polymorphs, we use a periodic graphs strategy by assembling "nodes" and "bridges" in 2D networks, in which "nodes" and "bridges" are represented by phosphorus atoms or clusters. This strategy has been widely used to predict new structures of crystals and metal organic frameworks (MOF).[81−83] Figure 1a illustrates the examples of

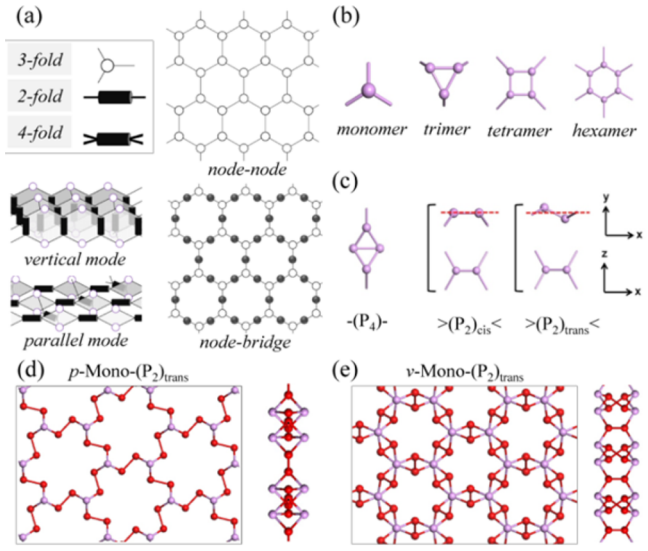

Figure 1. (a) Strategy to assemble "nodes" with 3-fold coordination and "bridges" with either 2-fold or 4-fold coordination into 2D topological networks. For 4-fold coordinated "bridge", both "vertical" and "parallel" modes are considered. (b) Phosphorus monomer, trimer, tetramer, and hexamer are chosen as four kinds of "nodes". (c) Phosphorus tetramer and dimer are chosen as 2- and 4-fold coordinated "bridges". The labels of "cis" and "trans" in 4-fold coordinated "chain" indicate two isomerized structures of phosphorus dimer. (d) and (e) Two examples of 2D phosphorus networks obtained by assembled with monomer "node" and $>(P_2)_{trans}<$ "chain" in parallel or vertical methods. Both purple and red balls here denote the phosphorus atoms. The red balls here illustrate the phosphorus atoms contributed by "chain".

one 3-coordinated "node" and two "bridges" with either 2- or 4-fold coordination, respectively; "node" can be connected by two proposed bridges or assembled directly to form 2D "networks". For 4-fold coordinated bridges, "vertical" and "parallel" modes are considered to build 2D networks, i.e., "bridges" are perpendicular or parallel to the 2D plane, as illustrated in Figure 1a. Varying "node" structures can extend the structure of 2D phosphorus allotropes.

Since phosphorus has typical 3-fold coordination, four types of nodes and two types of bridges are chosen to build 2D phosphorus crystalline networks, including phosphorus monomer, dimer, trimer, tetramer, and hexamer, shown in Figure 1b,c. Phosphorus timer, tetramer, and hexamer have ring-like structures that can be surrounded by three, four, and six neighbors, respectively. The 2-coordinated bridge is a phosphorus tetramer with quasi-tetrahedron structure, labeled

DOI: 10.1021/jacs.6b02964
J. Am. Chem. Soc. 2016, 138, 7091−7098

with "−(P_4)−". The 4-coordinated bridge is a phosphorus dimer with two isomerized structures, labeled with ">(P_2)$_{cis}$<" and ">(P_2)$_{trans}$<", respectively, as shown in Figure 1c. Therefore, 2D phosphorus allotropes based on these basic units can be categorized in two types defined with the nodes and bridges in 2D networks. Type I allotropes only contain nodes in 2D networks, named as "node−node *suffix*" that *"suffix"* is used to distinguish different arrangement of nodes if needed. Type II allotropes contain both "nodes" and "bridges", named as "*prefix*−node bridge". The *"prefix"* denotes the orientation of bridges in 2D networks, i.e., parallel or vertical to the 2D plane, labeled with "p" or "v", respectively. Figure 1d,e illustrates two examples of 2D phosphorus allotropes assembled with phosphorus monomer and ">(P_2)$_{trans}$<" bridge, i.e., p-Mono-(P_2)$_{trans}$ and v-Mono-(P_2)$_{trans}$, in which ">(P_2)$_{trans}$<" bridge is parallel and vertical to 2D plane, respectively. We conceive totally six Type I and 20 Type II 2D phosphorus allotropes based on four types of nodes and two types of bridges. The optimized structures are displayed in Figures S1−3 (see Supporting Information), and comprehensive details of their structural parameters, including symmetry, lattice constants, thickness, pore size, bond lengths and angles, are listed in Table S1 (see Supporting Information).

Type I Allotropes. As shown in Figures 2a and S1b, self-assembling of phosphorus monomers in PMNA and P-3M1

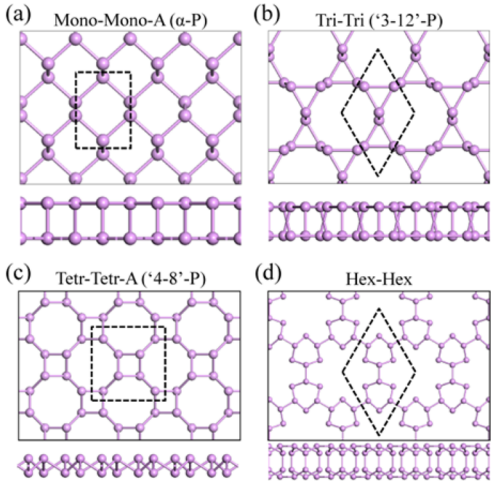

Figure 2. Top and side views of four Type I phosphorus allotropes are displayed, including (a) Mono−Mono-A (also α-P), (B) Tri−Tri (also '3−12'-P), (c) Tetr−Tetr-A (also '4−8'-P), and (d) Hex−Hex. The shapes of unit cell are labeled with a black dotted line.

symmetries brings two Type I phosphorus allotropes of Mono−Mono-A and Mono−Mono-B, which corresponds to black and blue phosphorene (α-P and β-P), respectively.[38,65] Meanwhile, Tri−Tri allotrope has the same structure as previously reported '3−12'-P, as shown in Figure 2b, where phosphorus atoms are packed in a mosaic of triangles and dodecagons. With 4-fold coordination, phosphorus tetramers can be assembled into two allotropes of Tetr−Tetr-A and Tetr−Tetr-B, which share same structures with '4−8'-P and ε-P, as shown in Figures 2c and S1e.[67,68] The tetramer-based allotropes have a mixture of quadrangles and octagons, and they can be converted to each other only by locally rotating P−P bonds in networks. In these allotropes, each node is surrounded by same number of neighbors as that of its coordination, and phosphorus atoms are packed in compacted 2D networks with the largest pore size of 5.55 Å in Tri−Tri allotrope. Differently, in Hex−Hex allotrope, each phosphorus hexamer is surrounded by three hexamers in plane, and the rest of the three dangling bonds are saturated by an underneath phosphorus hexamer, as shown in Figure 2d. In fact, the Hex−Hex allotrope can be looked at as a covalent bonded graphene bilayer in AA-stacking with each carbon atom replaced with phosphorus hexamer unit. Hex−Hex has the largest pore size of 7.16 Å in Type I phosphorus allotropes.

To evaluate the relative stability, their energies are calculated compared to the most stable phosphorene (α-P), as summarized in Table 1. Mono−Mono-B (β-P) is slightly less

Table 1. Relative Energy E_c (in unit of eV per atom), Band Gap E_g (in unit of eV), Number of Atoms in Unitcell*n*, and Young's Stiffness Y_s (in unit of N/m) of 2D Phosphorous Allotropes are Summarized

structure	E_c	E_{gap}(PBE/HSE06)	*n*	Y_s
Mono−Mono-A (α-P)	**0**	0.90/1.58 (D)	4	21, 91
Mono−Mono-B (β-P)	**0.002**	1.94/2.78 (I)	2	77
Tri−Tri ('3−12'-P)	0.121	0.92 (I)	6	
Tetr−Tetr-A ('4−8'-P)	**0.106**	1.96/2.82 (I)	8	
Tetr−Tetr-B (ε-P)	0.149	0.28 (D)	8	
Hex−Hex	**0.115**	0.97/1.96 (D)	24	52
p-Mono-(P_2)$_{cis}$	0.306	0.60 (I)	10	
p-Mono-(P_2)$_{trans}$	0.188	1.43 (I)	10	
v-Mono-(P_2)$_{cis}$	**0.098**	0.93/1.59 (I)	10	54
v-Mono-(P_2)$_{trans}$	**0.049**	1.44/2.15 (I)	10	47
p-Tri-(P_2)$_{cis}$	0.200	0.67 (I)	18	
p-Tri-(P_2)$_{trans}$	0.157	1.78 (I)	18	
v-Tri-(P_2)$_{cis}$	0.445	0.26 (I)	18	
v-Tri-(P_2)$_{trans}$	0.290	0.51 (I)	18	
p-Tetr-(P_2)$_{cis}$	0.195	0.70 (I)	24	
p-Tetr-(P_2)$_{trans}$	0.141	1.13 (I)	12	
v-Tetr-(P_2)$_{cis}$	0.367	0.17 (I)	24	
v-Tetr-(P_2)$_{trans}$	0.291	0.15 (I)	24	
p-Hex-(P_2)$_{cis}$	**0.083**	1.46/2.19 (D)	30	8
p-Hex-(P_2)$_{trans}$	**0.037**	1.97/2.78 (I)	30	10
v-Hex-(P_2)$_{cis}$	**0.039**	1.52/2.25 (I)	30	22
v-Hex-(P_2)$_{trans}$	**0.049**	1.86/2.68 (D)	30	27
Mono-(P_4)	**0.094**	2.55/3.42 (I)	14	2
Tri-(P_4)	0.180	1.93 (I)	18	
Tetr-(P_4)	**0.090**	1.99/2.83 (I)	24	2
Hex-(P_4)	0.160	1.49 (I)	18	
white phosphorus	**0.115**	4.93/6.15	4	

stable than α-P with energy of 0.002 eV per P atom, consistent with previous theoretical results.[65,69,70] In particular, Hex−Hex allotrope has the same energy per atom as that of white phosphorus molecular calculated at the same level (0.115 eV/P), which is more stable than Tetr−Tetr-B(ε-P) and Tri−Tri('3−12'-P) with energies of 0.149 and 0.121 eV, respectively.

Type II Allotropes. Introducing "bridges" into 2D crystalline network enriches the structures of 2D phosphorus allotrope family. Figure 3 displays eight Type II phosphorus allotropes that are more stable than white phosphorus ranked by the calculated energy. Other conceived structures are summarized in Figures S2 and S3. The 2-fold coordinated "−(P_4)−" bridges can be directly inserted between two neighboring nodes in the networks of Type I allotropes. Figure 3a,b displays the optimized structures of Mono-(P_4) and Tetr-

DOI: 10.1021/jacs.6b02964
J. Am. Chem. Soc. 2016, 138, 7091−7098

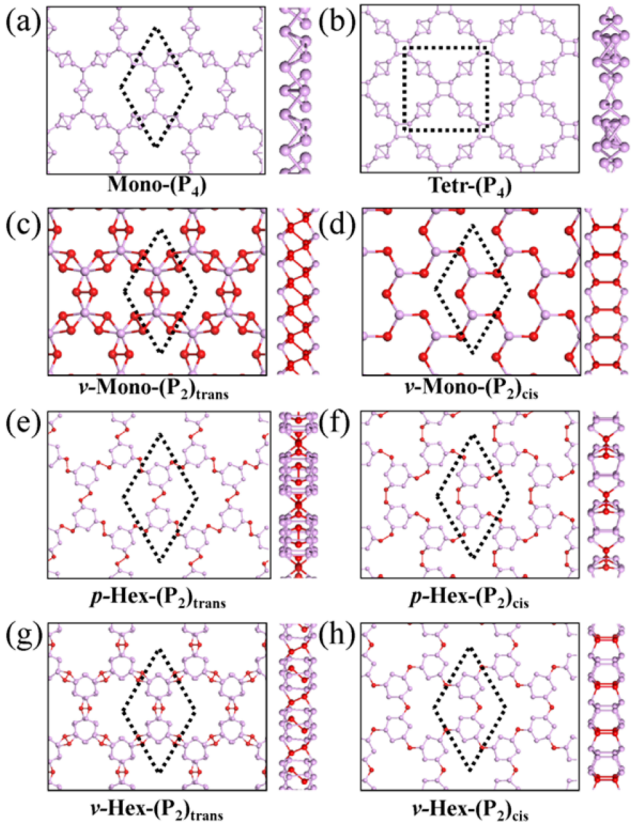

Figure 3. Top and side views of eight Type II phosphorus allotropes that are more stable than white phosphorus are displayed. The phosphorus atoms contributed by "bridges" and "nodes" are labeled with red and purple balls, respectively. The shapes of the unit cell are illustrated with black dotted lines.

(P_4) with P6 and P-42 M symmetries, respectively. The other two allotropes, i.e., Tri-(P_4) with P6 symmetry and Hex-(P_4) with P31 M symmetry, are displayed in Figure S3b,d. It is clear that inserting "bridges" into networks generally enlarges the pore size in 2D phosphorus allotropes. The diameters of pores in Mono-(P_4), Tri-(P_4), and Tetr-(P_4) are 9.07, 11.62, and 6.93 Å, respectively, which are significantly larger than those of Mono−Mono-A/B, Tri−Tri, and Tetr−Tetr-A/B allotropes. One exception is Hex-(P_4), which has smaller pores than Hex−Hex allotrope since each node is surround by six neighbors that are connected by a "−(P_4)−" bridge as in the former, while by three neighbors in the latter, as shown in Figure S 3d and 2d.

Different from the 2-fold coordinated "−(P_4)−" bridge, the ">$(P_2)_{cis\ or\ trans}$<" bridge with 4-fold coordination has two orientations when bridging four nodes, i.e., parallel or vertical to the plane. When ">$(P_2)_{cis\ or\ trans}$<" is vertical to the plane, 2D phosphorus allotropes have AA-stacked bilayer structures, and two layers are bonded with inner P−P bonds in ">(P_2)<" bridges. Figure 3c,f displays the optimized structures of v-Mono-$(P_2)_{cis\ or\ trans}$ and v-Hex-$(P_2)_{cis\ or\ trans}$, where "bridges" are labeled with red.

In contrary, 2D phosphorus allotropes with ">(P_2)<" parallel to the plane have compacted sandwich-like structures, where "nodes" in upper and lower layers are stacked in AA mode and ">(P_2)<" bridges are sandwiched between them. Figure 3g and 3h display the optimized structures of p-Hex-$(P_2)_{cis\ or\ trans}$. Similar with allotropes built with "−(P_4)−" bridges, Type II phosphorus allotropes with ">(P_2)<" bridges have large pores with the diameter ranging from 3.96 to 11.97 Å, where p-Hex-$(P_2)_{trans}$ has the largest size of pore, as shown in Figure 3g.

As summarized in Table 1, the calculated energy indicates that p-Hex-$(P_2)_{tans}$ is the most stable structure in all conceived allotropes with energy of 0.037 eV per P atom, and v-Hex-$(P_2)_{cis}$ is second stable with the energy of 0.039 eV per P atom. Although these structures are less stable than α-P, their energy is significantly smaller than white phosphorus (0.115 eV per P atom at same calculation level). Meanwhile, the calculated energy of other six allotropes, including Mono-(P_4), Tetr-(P_4), v-Mono-$(P_2)_{cis\ or\ trans}$, p-Hex-$(P_2)_{cis}$, and v-Hex-$(P_2)_{trans}$, ranges from 0.049 to 0.098 eV per P atom, which is also smaller than that of white phosphorus, indicating the possibility to obtain these allotropes in experiments.

To investigate the key factors to stabilize these new allotropes, we plot the deformation charge density, which is defined as the difference between the total charge density of 2D phosphorus allotropes and that of atoms, as shown in Figure S4. It can be found that P atoms are sp^3 hybridized with formation of strong covalent bonds with three neighboring phosphorus atoms, which majorly contribute to the stabilization of whole framework.

Dynamic Stability. The dynamic stability of nine 2D phosphorus allotropes that are more stable than white phosphorus, including Hex−Hex in Figure 2d and Type II allotropes in Figure 3, is confirmed with phonon spectrum calculations based on density functional perturbation theory. As shown in Figure S5, basically the phonon spectra show no imaginary phonon modes, suggesting that these nine 2D phosphorus allotropes are locally stable without any dynamic instability. The highest vibration frequency is 582 and 578 cm^{-1} for Mono-(P_4) and Tetr-(P_4) allotropes, respectively, significantly higher than those of the other seven 2D phosphorus allotropes. This behavior is due to the P−P bonds in "−(P_4)−" bridge.

Thermal Stability. In addition, the thermal stability at elevated temperature is another important indicator to test structure stability. For this purpose, BOMD is performed at DFT level for selected systems. The NVT ensemble is used. The initial structures are taken from the above optimized structures at zero temperature. The temperature of BOMD simulations are controlled at 300, 500, 700, 1000, 1200, and 1500 K. Snapshots at 5 ps for each allotrope are plotted at given temperatures, as shown in Figure S6. With NVT simulation, it can be seen that α- and β-P are stable up to temperature of 1000 K and are likely to break their structures at a temperature around 1200−1500 K, while the phase-change temperature is between 500 and 700 K for v-Mono-$(P_2)_{cis}$, 700 and 1000 K for v-Mono-$(P_2)_{trans}$, Mono-(P_4), Tetr-(P_4), and v-Hex-$(P_2)_{trans}$ allotropes, 1000 and 1200 K for p-Hex-$(P_2)_{cis}$ and p-Hex-$(P_2)_{trans}$, and 1200 and 1500 K for v-Hex-$(P_2)_{trans}$, respectively. One exception is Hex−Hex allotrope that changes phase when the temperature is over 300 K. The relative thermal stability of these allotropes is consistent with the calculated energy. Note that BOMD simulation here is artificial due to the limitation of simulation time scale and size of cells. Still, these results can indicate that most of these new low-energy 2D phosphorus allotropes are thermally stable above room temperature.

Mechanical Properties. The calculated elastic constants and Young's stiffness of the nine allotropes are summarized in Tables 1 and S3. As a benchmark, the elastic constants of C_{11}, C_{12}, C_{22}, and C_{44} of α-P are 103, 17, 24, and 24 N/m, consistent with previous results.[70] The Young's stiffness are anisotropic

DOI: 10.1021/jacs.6b02964
J. Am. Chem. Soc. 2016, 138, 7091−7098

with the values of 91 and 21 N/m. Taking the value of 5.55 Å as the thickness of α-P, the estimated Young's stiffness values are 164 and 38 GPa, respectively, agreeing well with previous theoretical values (166 and 44 GPa).[50] Differently, β-P has isotropic mechanic properties with $C_{11} = C_{22} = 78$ N/m and Young's stiffness of 77 N/m. Similar with β-P, nine new 2D phosphorus allotropes also have isotropic mechanical properties. The estimated elastic constant C_{11} is equal to C_{22} with the values ranging from 11 to 56 N/m, which are significantly smaller than those of β-P (78 N/m) and C_{11} of α-P (103 N/m). The calculated Young's stiffness of nine new 2D allotropes varies from 2 to 54 N/m. In particular, Mono-(P_4) and Tetr-(P_4) are the softest allotropes with the Young's modulus of 2 N/m, which are significantly smaller than α-P. It is clear that 2D phosphorus allotropes with large pore and "−(P_4)−" bridges have smaller values than those with smaller pores and ">(P_2)<" bridges.

Electronic Structure. The electronic band structures of all allotropes, together with density of states, are obtained at PBE calculation level, as shown in Figure S7. The calculated values of band gap are summarized in Table 1. It is clear that all of the considered 2D phosphorus allotropes are all semiconductors with the band gaps widely ranging from 0.15 to 2.55 eV. Only α-P, ε-P, Hex−Hex, p-Hex-$(P_2)_{cis}$, and v-Hex-$(P_2)_{trans}$ phosphorus allotropes are direct semiconductors, while others are indirect semiconductors. v-Hex-$(P_2)_{trans}$ has the largest direct band gap of 1.86 eV, and Mono-(P_4) allotrope has the largest indirect band gap of 2.55 eV at PBE calculation level.

Note that PBE always underestimates the band gaps of semiconductors. The electronic band structures of nine 2D phosphorus allotropes, which are more stable than white phosphorus, are calculated with the HSE06 screened hybrid density functional theory method, as shown in Figure 4. The calculated band gaps are summarized in Table 1. It is clear that the band gap of α-P is significantly underestimated at PBE calculation level (0.90 eV), while the HSE06 method increases this value to 1.58 eV, consisting with previous theoretical and experimental results.[41,69,70] For the direct-semiconducting 2D phosphorus allotropes, the band gap values are 1.69, 2.19, and 2.68 eV for Hex−Hex, p-Hex-$(P_2)_{cis}$, and v-Hex-$(P_2)_{trans}$ allotropes, respectively. Mono-(P_4) allotrope is an indirect semiconductor with the largest band gap of 3.42 eV. Generally, the HSE06 method increases the band gap by about 0.66−0.82 eV for phosphorus allotropes investigated here.

Typically, the interlayer interaction will affect the band structures of 2D materials. Our test calculations with DFT-D2 method on 2D phosphorus bilayer indicate that the interlayer interactions are weak with the values ranging from −11 to −39 meV per atom, and α-P bilayer has the largest interlayer interaction energy of −39 meV per atom. The optimized bilayer structures are displayed in Figure S8. The band gaps reduce from 0.06 to 0.93 eV, and β-P has the largest reduction of 0.93 eV in band gaps. The calculated band structures of nine 2D phosphorus allotropes are displayed in Figure S9, the interlayer interaction energy and band gap values are summarized in Table S2.

Band Alignments and Optical Properties. Our PBE calculation indicates that the work function of 2D phosphorus allotropes varies from 4.55 to 6.17 eV, as summarized in Table S4, and HSE06 calculation increases these values by about 0.4−0.5 eV. These values are close to the standard reduction potential of H^+/H_2 (−4.44 eV vs vacuum level (set as 0 eV)) and oxidation potential of O_2/H_2O (−5.67 eV vs vacuum level),[84] thus 2D phosphorus allotropes with moderate sizes of band gaps may be used for visible-light-driven overall water splitting. To elucidate this possibility, the energy position of valence band margin (VBM) and conduction band margin (CBM) are calculated at the HSE06 level, as shown in Figure 5a. It can be seen that the CBM and VBM of α-P are more positive than the reduction potential of H^+/H_2 and oxidation potential of O_2/H_2O, respectively, thus α-P can only be used as a visible-light-driven photocatalyst for hydrogen reduction in water splitting. Though both CBM and VBM of β-P match the hydrogen reduction potential and oxygen oxidation potential,

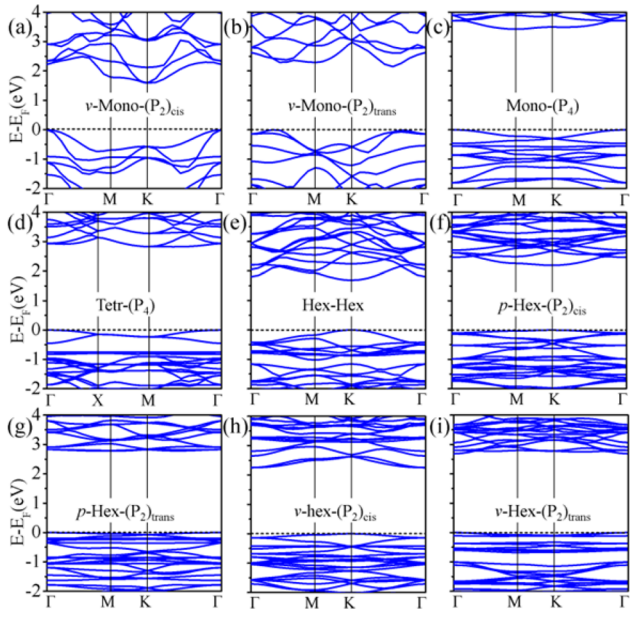

Figure 4. Band structures of nine phosphorus allotropes with the energy smaller than that of white phosphorus. The Fermi energy level is set to zero.

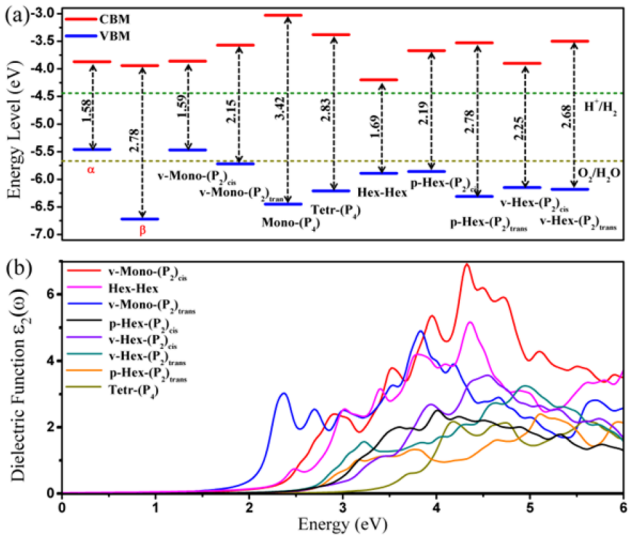

Figure 5. (a) The band alignment of 2D phosphorus allotropes calculated based on the HSE06 method. Vacuum level is set as 0 eV. The chemical reaction potentials for H^+/H_2 and O_2/H_2O are plotted with dotted lines. (b) The imaginary part of dielectric function of 2D phosphorus allotropes.

DOI: 10.1021/jacs.6b02964
J. Am. Chem. Soc. 2016, 138, 7091−7098

β-P is an indirect semiconductor with a wide band gap. Interestingly, except for v-Mono-$(P_2)_{cis}$, the calculated positions of VBM and CBM of other eight 2D phosphorus allotropes indicate that they have great possible potential to be used as element photocatalysts for visible-light-driven water splitting.

The optical adsorption spectra of 2D phosphorus allotropes are further examined with the HSE06 method. Figure 5b shows the computed imaginary part of the frequency-dependent dielectric function. We can see that the optical adsorption is fairly strong over a wide energy range between 2 and 5 eV, a range important for visible-light-driven water splitting.

Note that the band alignment is one fundamental requirement for photocatalysis water splitting; the performance also depends on the recombination of photoexcited electrons and holes and the microkinetic process of reaction on materials. The charge distribution profiles of CBM and VBM are plotted for 2D phosphorus allotropes, as shown in Figure S10, featuring the delocalized characteristics in these states and possible long diffusion distance of photoexcited electrons and holes. We also perform test calculations on p-Hex-$(P_2)_{trans}$ allotrope to investigate the microkinetic process of water splitting. The computation details can be found in Supporting Information. As shown in Figures S11−12, the calculated free energy profile of oxygen evolution reaction indicates that the irradiation of sample couple provide enough energy for water oxidation half reaction. Meanwhile, hydrogen evolution reaction can be driven with an ignorable external bias of 0.04 eV for the p-Hex-$(P_2)_{trans}$ allotrope. Moreover, since black phosphorene is sensitive to moisture,[85−87] the stability of 2D phosphorus allotropes in photocatalystic water splitting is another issue to be considered in practice. Experimentally, Favron et al. demonstrate that three environment parameters, i.e., oxygen, water, and visible light, are needed concurrently to induce the degradation of black phosphorene.[88] In particular, Wang et al. have recently reported the synthesis of water stable phosphorene via liquid exfoliation and demonstrate its application in photocatalytic oxygen generation and organic composition decomposition,[89] indicating one possible solution to overcome the stability problem of phosphorus allotropes in water splitting application.

Possible Fabrication Process. Due to their porous and multilayer structures, it is difficult to obtain them with normal experimental methods, such as chemical vapor deposition technique. However, some of them with lower energy may be synthesized with suitable pure phosphorus cluster via polyreaction reaction or P_nX_m (X = H or halogen atom) via polycondensation, as that in synthesis of covalent organic framework.[90,91]

Here, we choose white phosphorus molecule P_4 as an example unit. In polyreaction, P_4 molecules with ordering orientation in a 2D confined space or on substrate can be assembled into Tetr−Tetr-A ('4−8'-P) or Tetr-(P_4) allotropes with small energy barriers of 0.13 and 0.05 eV per atom with G-SSNEB method,[80] as shown in Figure 6, respectively. This value is significantly smaller than the transition energy barrier from α-P to β-P with the value of about 0.47 eV per atom.[65]

CONCLUSION

In conclusion, we proposed 21 2D phosphorus allotropes based on topological method and first-principles calculations. By assembling selected "nodes" and "bridges", represented by phosphorus monomer, dimer, trimer, tetramer, and hexamer, 2D phosphorus allotropes are built with tunable pores ranging from 3.87 to 11.97 Å. Nine new allotropes are predicted more stable than white phosphorus, ranked by the calculated energy. p-Hex-$(P_2)_{tans}$ is the most stable one in the conceived allotropes with the calculated energy of 0.037 eV per P atom compared with α-P. The vibration spectra calculation and BOMD simulation confirm both dynamic and thermal stabilities of these 2D allotropes. All conceived allotropes are semiconductors with a tunable band gap. v-Hex-$(P_2)_{trans}$ has the largest direct band gap of 2.68 eV at the HSE06 calculation level, which is larger than that of α-P (1.58 eV), and Mono-(P_4) has the largest indirect band gap of 3.42 eV. In particular, the band alignments of eight phosphorus allotropes match well with the chemical reaction potential of both H^+/H_2 and O_2/H_2O, indicating their potential application as element photocatalysts for visible-light-driven water splitting. Experimentally, some 2D phosphorus allotropes may be formed by phosphorus clusters or P_nX_m (X = H or halogen atom) via polyreaction or polycondensation.

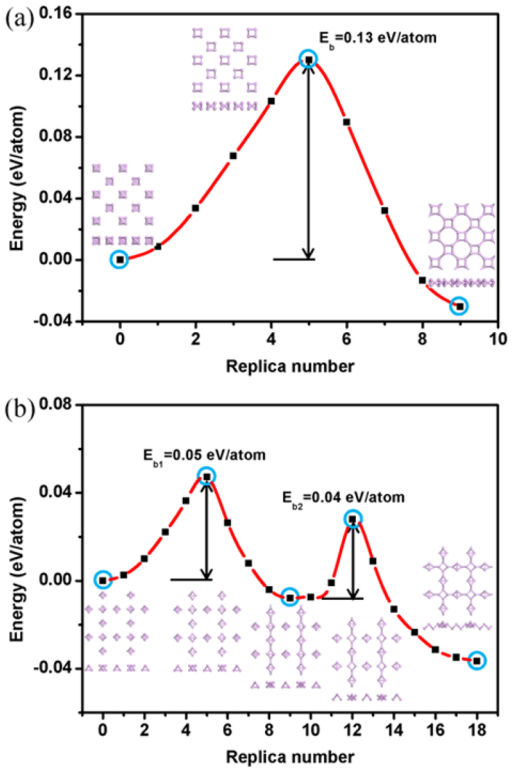

Figure 6. Minimum energy pathways of polyreaction from ordering P_4 units to (a) Tetr−Tetr-A (4−8) and (b) Tetr-(P_4) allotropes, respectively. The structures of initial, transition, and intermediate states are inserted. The phosphorus atoms are plotted with purple balls.

ASSOCIATED CONTENT

Supporting Information

The Supporting Information is available free of charge on the ACS Publications website at DOI: 10.1021/jacs.6b02964.

Optimized structures of conceived 2D phosphorus allotropes and details structural information including symmetry, lattice constants, thickness, diameter of pore, bond lengths and angles, elastic constants, band structures based on PBE calculations, phonon spectra of nine 2D allotropes, and snapshots of BOMD simulations, deformation charge density distribution profiles, optimized structures and band structures of

DOI: 10.1021/jacs.6b02964
J. Am. Chem. Soc. 2016, 138, 7091−7098

2D phosphorus allotrope bilayers, charge distribution of CBM and VBM, optimized structures and adsorption energies of (O, OH, H_2O, O_2, and OOH) on 2D phosphorus allotropes, and calculated free energy profiles of OER and HER on p-Hex-$(P_2)_{trans}$ are provided (PDF)

AUTHOR INFORMATION

Corresponding Author

*xjwu@ustc.edu.cn

Notes

The authors declare no competing financial interest.

ACKNOWLEDGMENTS

This work is partially supported by NSFC (21421063, 51172223, 21573204), by Strategic Priority Research Program of CAS (XDB01020300), the Fundamental Research Funds for the Central Universities (WK2060190025, WK2060140014, WK2310000053), by the National Key Basic Research Program (2012CB922001), by the National Program for Support of Top-notch Young Professional, the External Cooperation Program of BIC, Chinese Academy of Sciences, grant no. 211134KYSB20130017, and by USTCSCC, SCCAS, Tianjin, and Shanghai Supercomputer Centers.

REFERENCES

(1) Novoselov, K. S.; Geim, A. K.; Morozov, S. V.; Jiang, D.; Zhang, Y.; Dubonos, S. V.; Grigorieva, I. V.; Firsov, A. A. *Science* **2004**, *306*, 666.

(2) Lin, Y.; Connell, J. W. *Nanoscale* **2012**, *4*, 6908.

(3) Chhowalla, M.; Shin, H. S.; Eda, G.; Li, L.-J.; Loh, K. P.; Zhang, H. *Nat. Chem.* **2013**, *5*, 263.

(4) (a) Naguib, M.; Mochalin, V. N.; Barsoum, M. W.; Gogotsi, Y. *Adv. Mater.* **2014**, *26*, 992. (b) Anasori, B.; Xie, Y.; Beidaghi, M.; Lu, J.; Hosler, B. C.; Hultman, L.; Kent, P. R. C.; Gogotsi, Y.; Barsoum, M. W. *ACS Nano* **2015**, *9*, 9507.

(5) Enyashin, A. N.; Ivanovskii, A. L. *Phys. Status Solidi B* **2011**, *248*, 1879.

(6) Xu, L.-C.; Wang, R.-Z.; Miao, M.-S.; Wei, X.-L.; Chen, Y.-P.; Yan, H.; Lau, W.-M.; Liu, L.-M.; Ma, Y.-M. *Nanoscale* **2014**, *6*, 1113.

(7) Zhang, S.; Zhou, J.; Wang, Q.; Chen, X.; Kawazoe, Y.; Jena, P. *Proc. Natl. Acad. Sci. U. S. A.* **2015**, *112*, 2372.

(8) Yin, W.-J.; Xie, Y.-E.; Liu, L.-M.; Wang, R.-Z.; Wei, X.-L.; Lau, L.; Zhong, J.-X.; Chen, Y.-P. *J. Mater. Chem. A* **2013**, *1*, 5341.

(9) Sharma, B. R.; Manjanath, A.; Singh, A. K. *Sci. Rep.* **2014**, *4*, 7164.

(10) Hu, M.; Shu, Y.; Cui, L.; Xu, B.; Yu, D.; He, J. *Phys. Chem. Chem. Phys.* **2014**, *16*, 18118.

(11) Houssa, M.; Dimoulas, A.; Molle, A. *J. Phys.: Condens. Matter* **2015**, *27*, 253002.

(12) Acun, A.; Zhang, L.; Bampoulis, P.; Farmanbar, M.; van Houselt, A.; Rudenko, A. N.; Lingenfelder, M.; Brocks, G.; Poelsema, B.; Katsnelson, M. I.; Zandvliet, H. J. W. *J. Phys.: Condens. Matter* **2015**, *27*, 443002.

(13) Zhu, F.; Chen, W.; Xu, Y.; Gao, C.; Guan, D.; Liu, C.; Qian, D.; Zhang, S.-C.; Jia, J. *Nat. Mater.* **2015**, *14*, 1020.

(14) Zhang, S.; Yan, Z.; Li, Y.; Chen, Z.; Zeng, H. *Angew. Chem., Int. Ed.* **2015**, *54*, 3112.

(15) Kamal, C.; Ezawa, M. *Phys. Rev. B: Condens. Matter Mater. Phys.* **2015**, *91*, 085423.

(16) Wang, G.; Pandey, R.; Karna, S. P. *ACS Appl. Mater. Interfaces* **2015**, *7*, 11490.

(17) Cheng, L.; Liu, H.; Tan, X.; Zhang, J.; Wei, J.; Lv, H.; Shi, J.; Tang, X. *J. Phys. Chem. C* **2014**, *118*, 904.

(18) Kamal, C.; Chakrabarti, A.; Ezawa, M. *New J. Phys.* **2015**, *17*, 083014.

(19) Singh, D.; Gupta, S. K.; Lukačević, I.; Sonvane, Y. *RSC Adv.* **2016**, *6*, 8006.

(20) Li, Y.; Xu, L.; Liu, H.; Li, Y. *Chem. Soc. Rev.* **2014**, *43*, 2572.

(21) Malko, D.; Neiss, C.; Viñes, F.; Görling, A. *Phys. Rev. Lett.* **2012**, *108*, 086804.

(22) Maruyama, M.; Okada, S. *Appl. Phys. Express* **2013**, *6*, 095101.

(23) Terrones, H.; Terrones, M.; Hernández, E.; Grobert, N.; Charlier, J.-C.; Ajayan, P. M. *Phys. Rev. Lett.* **2000**, *84*, 1716.

(24) Tang, H.; Ismail-Beigi, S. *Phys. Rev. B: Condens. Matter Mater. Phys.* **2010**, *82*, 115412.

(25) Wu, X.; Dai, J.; Zhao, Y.; Zhuo, Z.; Yang, J.; Zeng, X. C. *ACS Nano* **2012**, *6*, 7443.

(26) Yu, X.; Li, L.; Xu, X.-W.; Tang, C.-C. *J. Phys. Chem. C* **2012**, *116*, 20075.

(27) Zhou, X.-F.; Dong, X.; Oganov, A. R.; Zhu, Q.; Tian, Y.; Wang, H.-T. *Phys. Rev. Lett.* **2014**, *112*, 085502.

(28) Penev, E. S.; Bhowmick, S.; Sadrzadeh, A.; Yakobson, B. I. *Nano Lett.* **2012**, *12*, 2441.

(29) Zhai, H.-J.; Kiran, B.; Li, J.; Wang, L.-S. *Nat. Mater.* **2003**, *2*, 827.

(30) Tai, G.; Hu, T.; Zhou, Y.; Wang, X.; Kong, J.; Zeng, T.; You, Y.; Wang, Q. *Angew. Chem.* **2015**, *127*, 15693.

(31) Mannix, A. J.; Zhou, X.-F.; Kiraly, B.; Wood, J. D.; Alducin, D.; Myers, B. D.; Liu, X.; Fisher, B. L.; Santiago, U.; Guest, J. R.; Yacaman, M. J.; Ponce, A.; Oganov, A. R.; Hersam, M. C.; Guisinger, N. P. *Science* **2015**, *350*, 1513.

(32) Feng, B.; Zhang, J.; Zhang, Q.; Li, W.; Li, S.; Li, H.; Cheng, P.; Meng, S.; Chen, L.; Wu, K. H. *Nat. Chem.* **2016**, DOI: 10.1038/nchem.2491.

(33) Hultgren, R.; Gingrich, N. S.; Warren, B. E. *J. Chem. Phys.* **1935**, *3*, 351.

(34) Okudera, H.; Dinnebier, R. E.; Simon, A. *Z. Kristallogr. - Cryst. Mater.* **2005**, *220*, 259.

(35) Thurn, V. H.; Krebs, H. *Acta Crystallogr., Sect. B: Struct. Crystallogr. Cryst. Chem.* **1969**, *25*, 125.

(36) Ruck, M.; Hoppe, D.; Wahl, B.; Simon, P.; Wang, Y.; Seifert, G. *Angew. Chem., Int. Ed.* **2005**, *44*, 7616.

(37) Bachhuber, F.; von Appen, J.; Dronskowski, R.; Schmidt, P.; Nilges, T.; Pfitzner, A.; Weihrich, R. *Angew. Chem., Int. Ed.* **2014**, *53*, 11629.

(38) Liu, H.; Neal, A. T.; Zhu, Z.; Luo, Z.; Xu, X.; Tománek, D.; Ye, P. D. *ACS Nano* **2014**, *8*, 4033.

(39) Koenig, S. P.; Doganov, R. A.; Schmidt, H.; Castro Neto, A. H.; Özyilmaz, B. *Appl. Phys. Lett.* **2014**, *104*, 103106.

(40) Li, L.; Yu, Y.; Ye, G. J.; Ge, Q.; Ou, X.; Wu, H.; Feng, D.; Chen, X. H.; Zhang, Y. *Nat. Nanotechnol.* **2014**, *9*, 372.

(41) Sa, B.; Li, Y.-L.; Qi, J.; Ahuja, R.; Sun, Z. *J. Phys. Chem. C* **2014**, *118*, 26560.

(42) Kou, L.; Chen, C.; Smith, S. C. *J. Phys. Chem. Lett.* **2015**, *6*, 2794.

(43) Rodin, A. S.; Carvalho, A.; Castro Neto, A. H. *Phys. Rev. Lett.* **2014**, *112*, 176801.

(44) Fei, R.; Yang, L. *Nano Lett.* **2014**, *14*, 2884.

(45) Xu, Y.; Dai, J.; Zeng, X. C. *J. Phys. Chem. Lett.* **2015**, *6*, 1996.

(46) Qin, G.; Yan, Q.-B.; Qin, Z.; Yue, S.-Y.; Cui, H.-J.; Zheng, Q.-R.; Su, G. *Sci. Rep.* **2014**, *4*, 6946.

(47) Ong, Z.-Y.; Cai, Y.; Zhang, G.; Zhang, Y.-W. *J. Phys. Chem. C* **2014**, *118*, 25272.

(48) Jain, A.; McGaughey, A. J. H. *Sci. Rep.* **2014**, *5*, 8501.

(49) Fei, R.; Faghaninia, A.; Soklaski, R.; Yan, J.-A.; Lo, C.; Yang, L. *Nano Lett.* **2014**, *14*, 6393.

(50) Wei, Q.; Peng, X. *Appl. Phys. Lett.* **2014**, *104*, 251915.

(51) Wang, L.; Kutana, A.; Zou, X.; Yakobson, B. I. *Nanoscale* **2015**, *7*, 9746.

(52) Jiang, J.-W.; Park, H. S. *Nat. Commun.* **2014**, *5*, 4727.

(53) Jiang, J.-W.; Park, H. S. *J. Phys. D: Appl. Phys.* **2014**, *47*, 385304.

(54) Liu, Q.; Zhang, X.; Abdalla, L. B.; Fazzio, A.; Zunger, A. *Nano Lett.* **2015**, *15*, 1222.

(55) Ge, Y.; Wan, W.; Yang, F.; Yao, Y. *New J. Phys.* **2015**, *17*, 035008.

DOI: 10.1021/jacs.6b02964
J. Am. Chem. Soc. 2016, 138, 7091−7098

(56) Li, L.; Ye, G. J.; Tran, V.; Fei, R.; Chen, G.; Wang, H.; Wang, J.; Watanabe, K.; Taniguchi, T.; Yang, L.; Chen, X. H.; Zhang, Y. *Nat. Nanotechnol.* **2015**, *10*, 608.
(57) Sun, J.; Zheng, G.; Lee, H.-W.; Liu, N.; Wang, H.; Yao, H.; Yang, W.; Cui, Y. *Nano Lett.* **2014**, *14*, 4573.
(58) (a) Zhao, S.; Kang, W.; Xue, J. *J. Mater. Chem. A* **2014**, *2*, 19046. (b) Li, W.; Yang, Y.; Zhang, G.; Zhang, Y.-W. *Nano Lett.* **2015**, *15*, 1691.
(59) Zhang, R.; Wu, X.; Yang, J. *Nanoscale* **2016**, *8*, 4001.
(60) Sun, J.; Lee, H.-W.; Pasta, M.; Yuan, H.; Zheng, G.; Sun, Y.; Li, Y.; Cui, Y. *Nat. Nanotechnol.* **2015**, *10*, 980.
(61) (a) Kulish, V. V.; Malyi, O. I.; Persson, C.; Wu, P. *Phys. Chem. Chem. Phys.* **2015**, *17*, 13921. (b) Liu, X.; Wen, Y.; Chen, Z.; Shan, B.; Chen, R. *Phys. Chem. Chem. Phys.* **2015**, *17*, 16398.
(62) Dai, J.; Zeng, X. C. *J. Phys. Chem. Lett.* **2014**, *5*, 1289.
(63) Ganesan, V. D. S/O; Zhang, C.; Feng, Y. P.; Shen, L. *arXiv.org, e-Print Arch., Condens. Matter* **2015**, *1507*, 07343.
(64) Kou, L.; Frauenheim, T.; Chen, C. *J. Phys. Chem. Lett.* **2014**, *5*, 2675.
(65) Zhu, Z.; Tománek, D. *Phys. Rev. Lett.* **2014**, *112*, 176802.
(66) Guan, J.; Zhu, Z.; Tománek, D. *Phys. Rev. Lett.* **2014**, *113*, 046804.
(67) Guan, J.; Zhu, Z.; Tománek, D. *ACS Nano* **2014**, *8*, 12763.
(68) Wu, M.; Fu, H.; Zhou, L.; Yao, K.; Zeng, X. C. *Nano Lett.* **2015**, *15*, 3557.
(69) Zhao, T.; He, C. Y.; Ma, S. Y.; Zhang, K. W.; Peng, X. Y.; Xie, G. F.; Zhong, J. X. *J. Phys.: Condens. Matter* **2015**, *27*, 265301.
(70) Liu, J.; Guo, Y.; Zhang, S.; Wang, Q.; Kawazoe, Y.; Jena, P. *J. Phys. Chem. C* **2015**, *119*, 24674.
(71) Yu, G.; Jiang, L.; Zheng, Y. *J. Phys.: Condens. Matter* **2015**, *27*, 255006.
(72) He, C.; Zhang, C.; Ouyang, T.; Li, J.; Zhong, J. *arXiv.org, e-Print Arch., Condens. Matter* **2016**, *1602*, 05734.
(73) Wang, F.; Ng, W. K. H.; Yu, J. C.; Zhu, H.; Li, C.; Zhang, L.; Liu, Z.; Li, Q. *Appl. Catal., B* **2012**, *111−112*, 409.
(74) (a) Kresse, G.; Hafner, J. *Phys. Rev. B: Condens. Matter Mater. Phys.* **1993**, *47*, 558. (b) Kresse, G.; Hafner, J. *Phys. Rev. B: Condens. Matter Mater. Phys.* **1994**, *49*, 14251. (c) Kresse, G.; Furthmüller, J. *Comput. Mater. Sci.* **1996**, *6*, 15. (d) Kresse, G.; Furthmüller, J. *Phys. Rev. B: Condens. Matter Mater. Phys.* **1996**, *54*, 11169.
(75) (a) Blöchl, P. E. *Phys. Rev. B: Condens. Matter Mater. Phys.* **1994**, *50*, 17953. (b) Kresse, G.; Joubert, D. *Phys. Rev. B: Condens. Matter Mater. Phys.* **1999**, *59*, 1758.
(76) Perdew, J. P.; Burke, K.; Ernzerhof, M. *Phys. Rev. Lett.* **1996**, *77*, 3865.
(77) (a) Heyd, J.; Scuseria, G. E.; Ernzerhof, M. *J. Chem. Phys.* **2003**, *118*, 8207. (b) Paier, J.; Marsman, M.; Hummer, K.; Kresse, G.; Gerber, I. C.; Ángyán, J. G. *J. Chem. Phys.* **2006**, *124*, 154709.
(78) Clark, S. J.; Segall, M. D.; Pickard, C. J.; Hasnip, P. J.; Probert, M. I. J.; Refson, K.; Payne, M. C. *Z. Kristallogr. - Cryst. Mater.* **2005**, *220*, 567.
(79) Grimme, S. *J. Comput. Chem.* **2006**, *27*, 1787.
(80) Sheppard, D.; Xiao, P.; Chemelewski, W.; Johnson, D. D.; Henkelman, G. *J. Chem. Phys.* **2012**, *136*, 074103.
(81) Smith, J. V.; Dytrych, W. J. *Nature* **1984**, *309*, 607.
(82) Delgado Friedrichs, O.; Dress, A. W. M.; Huson, D. H.; Klinowski, J.; Mackay, A. L. *Nature* **1999**, *400*, 644.
(83) Delgado Friedrichs, O.; O'Keeffe, M.; Yaghi, O. M. *Acta Crystallogr., Sect. A: Found. Crystallogr.* **2003**, *59*, 22.
(84) Chakrapani, V.; Angus, J. C.; Anderson, A. B.; Wolter, S. D.; Stoner, B. R.; Sumanasekera, G. U. *Science* **2007**, *318*, 1424.
(85) Wood, J. D.; Wells, S. A.; Jariwala, D.; Chen, K.-S.; Cho, E. K.; Sangwan, V. K.; Liu, X.; Lauhon, L. J.; Marks, T. J.; Hersam, M. C. *Nano Lett.* **2014**, *14*, 6964.
(86) Favron, A.; Gaufrès, E.; Fossard, F.; Phaneuf-L'Heureux, A.-L.; Tang, N. Y-W.; Lévesque, P. L.; Loiseau, A.; Leonelli, R.; Francoeur, S.; Martel, R. *Nat. Mater.* **2015**, *14*, 826.
(87) Island, J. O.; Steele, G. A.; van der Zant, H. S. J.; Castellanos-Gomez, A. *2D Mater.* **2015**, *2*, 011002.
(88) Wang, G.; Slough, W. J.; Pandey, R.; Karna, S. P. *2D Mater.* **2016**, *3*, 025011.
(89) Wang, H.; Yang, X.; Shao, W.; Chen, S.; Xie, J.; Zhang, X.; Wang, J.; Xie, Y. *J. Am. Chem. Soc.* **2015**, *137*, 11376.
(90) Kuhn, P.; Antonietti, M.; Thomas, A. *Angew. Chem., Int. Ed.* **2008**, *47*, 3450.
(91) Côté, A. P.; Benin, A. I.; Ockwig, N. W.; O'Keeffe, M.; Matzger, A. J.; Yaghi, O. M. *Science* **2005**, *310*, 1166.

DOI: 10.1021/jacs.6b02964
J. Am. Chem. Soc. 2016, 138, 7091−7098